rals. Two-, three-, and four-armed spirals can also be produced, depending on the initial conditions (*11*). All these structures are remarkably stable, except for colliding wave fronts of independent origin, which neither penetrate through nor reflect off each other but rather result in mutual annihilation on contact. Our computer model easily generates all these features.

Our algorithm operates on an initially homogeneous hexagonal grid. Initial conditions are set up such that one or more cells are "activated" while others are either "quiescent" or "receptive." In the next time step the activated cells may then stimulate (catalyze) the immediately adjacent cells into activity. The probability that this reaction is completed in one time step is governed by the first parameter, designated productivity. Propagation of activity is restricted by the second parameter, which specifies a period during which a cell must remain quiescent after stimulation. Cells cannot be propagated into during this quiescent phase, nor while they themselves are active. The active phase lasts one time step.

With the probability of propagation set to unity and the quiescent time set to two time steps, the following initial conditions give rise to the structures shown in Fig. 1.

1) An isolated active cell produces a single, circularly symmetric, expanding wavelike front of activity.

2) A single active cell buffered by an adjacent quiescent cell gives rise to a recurring series of concentric wavelike rings.

3) The end points of a line of activated cells buffered on one side by a line of quiescent cells give rise to growing one-armed spiral patterns.

4) The contact point between two lines of activated cells placed end to end but buffered on opposite sides by quiescent cells produces two-armed spiral patterns.

5) Multiarmed spirals (three or more arms) are generated by lines of buffered activators meeting at a common central cell.

These basic structures are extremely stable. When wave fronts from various centers meet, the fronts do indeed annihilate each other, but the structures internal to these surfaces of contact persist throughout the simulation. The only notable variation is illustrated by the time sequence, which shows that the spirals are intermittently connected and disconnected in the core region, as is also observed in active, excitable chemical media (*11*).

Given that the reaction is likely to occur, there is in fact only one free parameter in our model, the quiescent time. It should be emphasized that this parameter does not in any way affect the variety of forms that result but controls only the scaling of the features, such as the interarm separation in fully matured spiral patterns. Thus, the periodicity in these wavelike structures is intrinsic to the diffusion-reaction time scale of the chemical system. Specifically, it is not dependent on the properties of an unspecified local oscillator, nor are the patterns dependent on boundary conditions, of which there are none in this particular simulation. However, any inert boundary in this simulation, as in the chemical reactions, limits only the extent of the propagation.

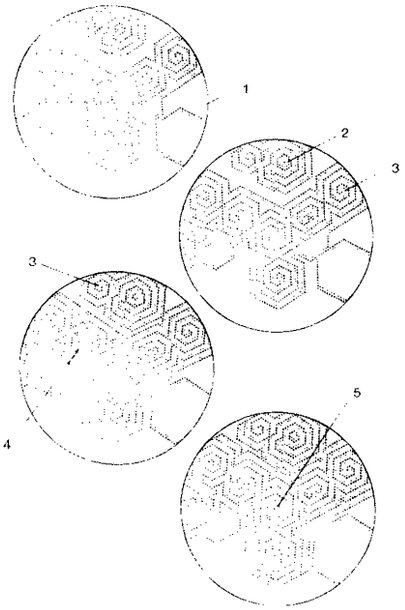

Fig. 1. Sequential time steps in the computer modeling of the Belousov-Zhabotinsky reaction. The structures numbered 1 to 5 result from the initial conditions described in the text.

We hope that these simulations will lead researchers to regard such self-organizing structures as the expected consequences of a wide class of propagating and autocatalytic reactions that can be easily modeled. This broad class, we believe, includes not only the chemical reactions described above but also morphologically equivalent growth patterns in slime molds, certain stages of embryonic development, and the shock-driven models of spiral arm development in galactic systems.

BARRY F. MADORE
WENDY L. FREEDMAN
David Dunlap Observatory,
Department of Astronomy,
University of Toronto,
Toronto, Ontario, Canada M5S 1A5

References and Notes

1. W. L. Freedman and B. F. Madore, *Astrophys. J.* **265**, 140 (1983).
2. B. P. Belousov, *Sb. Ref. Radiats. Med. 1958*, 145 (1959); A. M. Zhabotinsky, *Dokl. Akad. Nauk SSSR* **157**, 392 (1964).
3. A. T. Winfree, *Science* **175**, 634 (1972).
4. G. Nicolis and I. Prigogine, *Self-Organization in Non-Equilibrium Systems* (Wiley, New York, 1977).
5. A. N. Zaikin and A. M. Zhabotinsky, *Nature (London)* **225**, 535 (1970).
6. P. Hanusse, *C. R. Acad. Sci. Ser. C* **277**, 263 (1973).
7. J. Stanshine, thesis, Massachusetts Institute of Technology (1975).
8. J. F. Tyson, *Ann. N.Y. Acad. Sci.* **316**, 279 (1979).
9. D. S. Cohen, J. C. Neu, R. R. Rosales, *SIAM (Soc. Ind. Appl. Math.) J. Appl. Math.* **39**, 8 (1978).
10. A. T. Winfree, *Sci. Am.* **230**, 82 (June 1974).
11. K. I. Agladze and V. I. Krinsky, *Nature (London)* **296**, 424 (1982).
12. This work was supported in part by the Natural Sciences and Engineering Research Council of Canada, Zonta International, and the University of Toronto. We thank S. Shore for helpful comments and for access to his encyclopedic store of references.

6 April 1983; revised 6 April 1983

Phaeodarian Skeletons: Their Role in Silica Transport to the Deep Sea

Abstract. *The skeletons of phaeodarian Radiolaria transport and redistribute silica to the tropical deep oceans by dissolving in the water column and on the sea floor. The skeletons are initially solid but within a few days to months become progressively more porous while settling through the water column. Phaeodarian Radiolaria are rarely preserved in the bottom sediments; in contrast, polycystine Radiolaria are the dominant Radiolaria preserved in the fossil record. This preservational difference may be due to differences in skeletal constituents.*

Phaeodarian Radiolaria are marine protozoans that are ubiquitous throughout the water column in the pelagic environment (*1, 2*), but their skeletons are commonly absent in marine sediments (*3*) and are much less well preserved than those of polycystine Radiolaria (*4, 5*). The skeletons of Phaeodaria are reported to be composed of an admixture of silica and organic matter (*2*); the organic content and the construction of silica into hollow bars (*3*) or porous skeletons (*2, 6*) are supposedly responsible for the poor preservation. We present new findings about the vertical mass flux of Phaeodaria together with observations

on the differences in skeletal micro- and ultrastructure between phaeodarian and polycystine Radiolaria. These results suggest that (i) the actual mass flux of Phaeodaria as measured by sediment-trap experiments is a significant input term for silica recycling in tropical oceans, (ii) phaeodarian skeletal ultrastructure strongly controls dissolution and thus the degree to which silica from skeletons will be recycled in the water column and at the sediment-water interface, and (iii) there is only a small amount of organic matter present within the phaeodarian skeletons.

The vertical flux of Phaeodaria at the equatorial Atlantic and Panama Basin PARFLUX sediment-trap stations (*7*) ranged from 6 to 8 percent of the total number of radiolarian skeletons and 3 to 23 percent of the total silica mass flux. These are probably minimal values because of the relatively poor in situ preservation of the phaeodarian skeletons in the traps. Larger flux values are likely in environments where phaeodarian species predominate (*4*). In tropical oceans, since Radiolaria form the bulk of the silica flux (*8*) as well as suspension (*9*), the Phaeodaria should contribute a sizable vertical flux, especially since the skeletal dissolution of phaeodarians is much faster (*4*) than that of polycystines.

Skeletons of Phaeodaria have a fundamentally different structure from those of Polycystina. *Challengeron willemoesii*, a typical shallow-dwelling phaeodarian (Fig. 1), represents an internal skeletal morphology that is common to all 18 species of the family Challengeridae that we investigated with one exception (*8*). The microstructural units, as revealed by partial dissolution, are amphorae or wine bottle–shaped structures about 3 to 3.5 μm in diameter that appear to be cemented with more readily soluble silica; this structural arrangement makes it possible for the amphorae to be freed from their skeletal integrity as dissolution proceeds (Fig. 1).

Specimens collected in plankton tows in the Panama Basin and not subjected to dissolution after retrieval (*10*) revealed a relatively uniform and nearly solid skeletal structure (Fig. 1c). The same species from sediment traps show varying degrees of dissolution porosity resulting from removal of the amphora-cementing material which is composed of numerous tubes (Fig. 1d). The amphorae are only slightly dissolved at this stage. The effects of dissolution are shown by increasing skeletal porosity and decreasing numbers of *C. willemoesii* with increasing depth (*8*). In contrast, the flux of polycystine (Spumellaria and Nassellaria) skeletons is essentially constant with depth; most of the polycystine populations found at the sea surface (over 200 species at a given station) reach the sea floor, where many of them also dissolve prior to burial (*8*). According to a laboratory sinking speed experiment in 3°C seawater, *C. willemoesii* settles 20 m/day and should require 250 days to settle through a 5-km water column (*11*). About a year would be required for a silica particle 0.1 μm thick to dissolve at 3°C (*12*). Thus, the drastic decrease of flux of this species with increasing trap depth is also consistent with both the sinking speed and estimated dissolution rate data (*4*), especially in view of the fact that the entire skeleton appears to become porous at once, as compared with polycystines which become porous more gradually, starting from the outside (*12*).

The adsorption of the acid-base indicator methyl red into these skeletons can be used to obtain a semiquantitative measure of the porosity and specific surface area (*12*) and to observe differences in the intensity of dye adsorption. The type of porosity shown in Figs. 1d and 2d always corresponds to greater stain intensity; skeletons showing no staining also exhibit little or no available porosity when viewed with transmission electron microscopy at high magnification.

Haeckeliana porcellana, a common large phaeodarian (*13*), also shows porous skeletons (Fig. 2) characterized by a tubular configuration which probably originated during growth and is a secondary dissolution feature. Many castanellid species, a group closely related to *H. porcellana*, from plankton net tows show relatively solid skeletons whereas sediment-trap specimens show varying degrees of porosity, and thus probably the skeletons of *H. porcellana* were initially more solid. The estimated sinking speed of *H. porcellana* is such that they should require about 12 days to settle through a

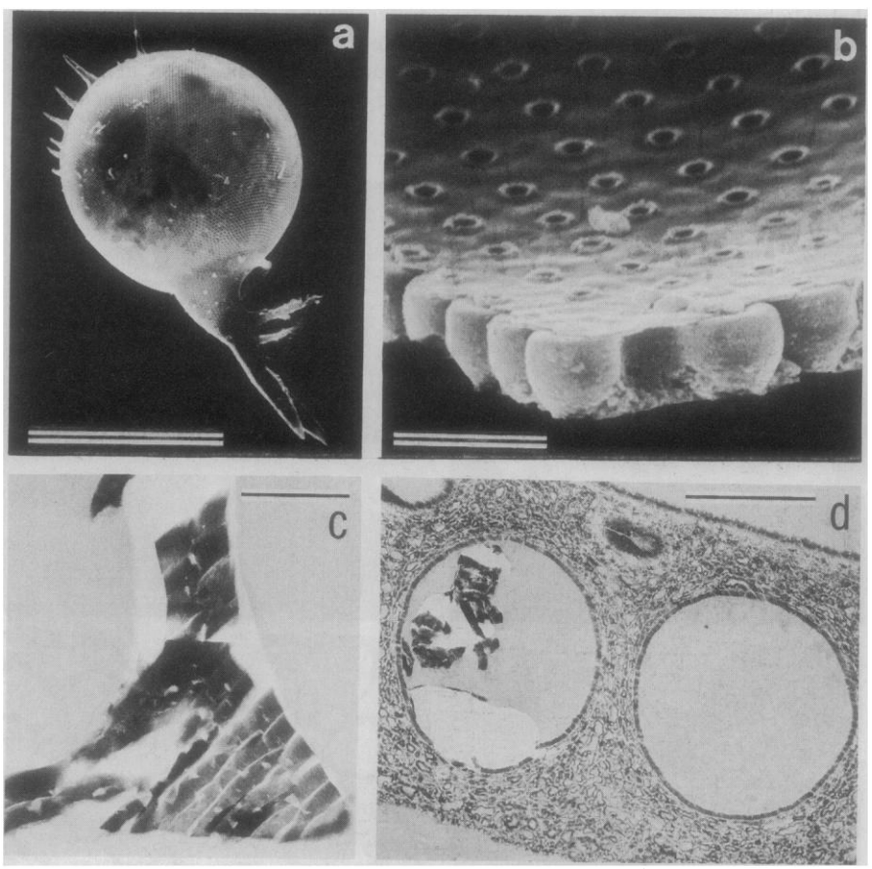

Fig. 1. (a) Scanning electron micrograph of a specimen of *Challengeron willemoesii* Haeckel recovered from the Panama Basin station (PB) (5°21′N, 81°53′W) trap, 667 m; scale bar, 200 μm. (b) An oblique view (scanning electron microscopy) of the shell wall of an intentionally broken specimen (PB trap, 1268 m; scale bar, 5 μm). Basic skeletal units are siliceous amphora-shaped structures cemented by granular silica. The amphorae are secured to a siliceous matrix with their necks oriented toward the inside of the shell. (c) Transmission electron micrograph of an enlarged cross section of an intact specimen that was immediately dried on board to retard dissolution (PB, 0 to 100 m, plankton tow; scale bar, 1 μm). Parallel cracks are an artifact of thin sectioning; the knife cut from lower right to upper left, and several chips fell out. Note the small angular pores, which have not been found in polycystine skeletons (*12*). (d) Transmission electron micrograph of a sample that has undergone dissolution (PB trap, 667 m; scale bar, 2 μm). The pores in (d) are larger and more numerous than in (c), and the material itself has become a tubular matrix; the white circles are amphorae in cross section.

5-km water column (*11*). Probably this species reaches the bottom without much alteration but develops the above described structures in the sediment traps.

Haeckeliana porcellana and other large phaeodarians (for example, castanellids, 13 to 24 μg per shell; sinking speed, 53 to 384 m/day) appear to be the major fast carriers of large quantities of silica per individual shell. These weight values are two to three orders of magnitude greater (*11*) than those of Quaternary radiolarians (*14*). The skeletal weight difference between biocoenoses, represented by the above typical large phaeodarians and the Quaternary polycystine radiolarians, is attributed to selective dissolution of soluble species. The large phaeodarians, whose influence on dissolved silicon in the deep waters is significant, can be used to monitor silica cycling in certain pelagic environments.

We do not know how much organic matter is admixed with silica in phaeodarian skeletons. However, when the skeletal ultramorphology of several species of Phaeodaria was observed with transmission electron microscopy before and after ashing at 500°C for 3 hours, no obvious changes were observed at magnifications of up to ×100,000. This finding suggests that organic matter does not account for a significant volume of the skeleton.

Of the few phaeodarians preserved in the fossil record (*3*), we have studied specimens of two *Lithogromia* species from the Deep Sea Drilling Program cores (site 203, Pleistocene in age). These have a morphology similar to that of *C. willemoesii*, but the skeletal pores apparently caused by dissolution are different. In addition to having a pore size similar to the tube size in the sediment-trap phaeodarians (~ 500 Å in diameter; Figs. 1 and 2), they have much smaller secondary pores (~ 50 Å). This size is similar to that in polycystines recovered from the sediments (*12*) and developed in the walls of the tubes. These small pores could have resulted from dissolution of silica and surface coating by some elements that occurred in sediments. A thin outer porous layer in polycystine skeletons first develops during settling in the water column and then spreads into the center of the skeletons in sea-floor environments (*12*). The pores in the outer layer do not seem to increase in size nor do they fall off, perhaps an indication that some sort of coating process may be taking place to retard the dissolution. It is feasible that cations such as iron, aluminum, and manganese are present in the skeletal surface (*15*), reducing solubility.

These observations suggest that phaeodarian skeletons may have a different, possibly a more hydrated silica, composition from polycystine skeletons. As a result, phaeodarians quickly become porous and increase the skeletal surface area exposed to seawater within a few days to months in the water column, while polycystines do not.

KOZO TAKAHASHI
Scripps Institution of Oceanography, University of California, San Diego, La Jolla 92093

DAVID C. HURD
Shell Development Company, Houston, Texas 77001

SUSUMU HONJO
Woods Hole Oceanographic Institution, Woods Hole, Massachusetts 02543

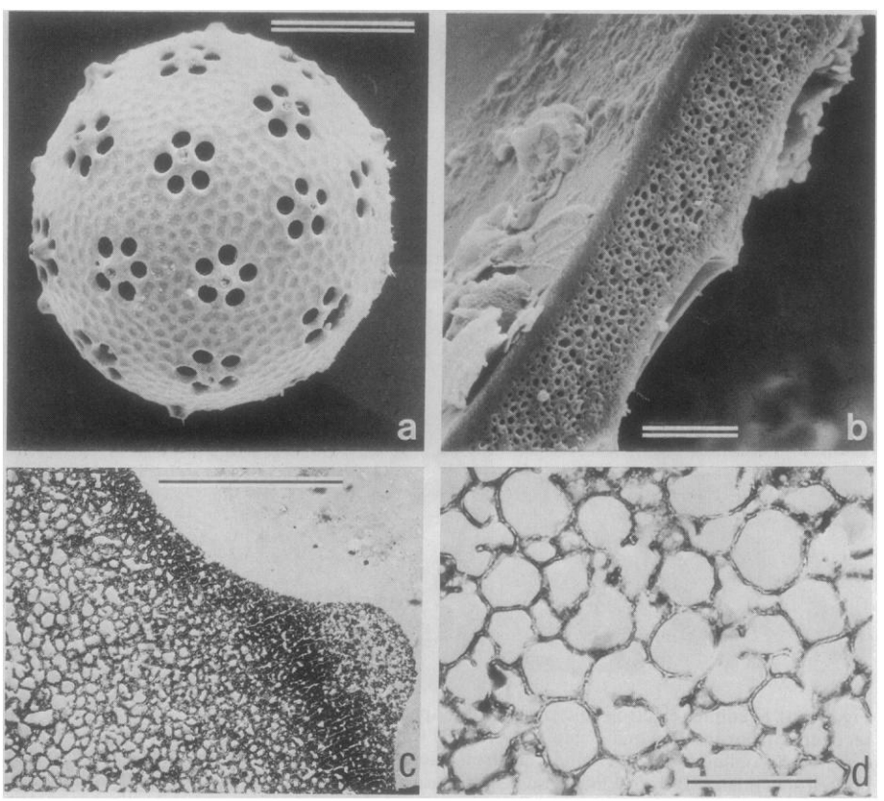

Fig. 2. (a) Scanning electron micrograph of a specimen of *Haeckeliana porcellana* Haeckel recovered from the station E (13°30.2′N, 54°00.1′W) trap, 988 m; scale bar, 100 μm. (b) Cross section (scanning electron microscopy) of the shell wall (station E, trap, 988 m; scale bar, 5 μm). (c) Complimentary transmission electron micrograph to (b) [central Pacific station (P_1) (15°21.1′N, 151°28.5′W) trap, 978 m; scale bar, 5 μm]. The tubes within the skeleton in (b) are hollow. (d) An enlarged view of (c), showing the tubular structure more clearly (station P_1 trap, 978 m; scale bar, 1 μm).

References and Notes

1. V. V. Reshetnyak, *Tr. Zool. Inst. Akad. Nauk SSSR* **21**, 94 (1955); *Deep-Sea Phaeodarian Radiolaria of the Northwest Pacific* (Fauna SSSR, new series 94, Zoological Institute, Academy of Sciences of the U.S.S.R., Moscow, 1966).
2. E. Haeckel, *Rep. Voy. Challenger Zool.* **18**, 1 (1877).
3. W. R. Riedel, in *The Sea* (Wiley, New York, 1963), vol. 3, pp. 866–887; C. J. Stadum and H. Y. Ling, *Micropaleontology* **15**, 481 (1969); P. Dumitrica, *Initial Rep. Deep Sea Drill. Proj.* **21**, 751 (1973); W. H. Berger, *Chem. Oceanogr.* **5**, 265 (1976).
4. J. Erez, K. Takahashi, S. Honjo, *Earth Planet. Sci. Lett.* **59**, 245 (1982); D. C. Hurd and K. Takahashi, *Mar. Micropaleontol.* **7**, 441 (1983).
5. W. H. Berger, *Science* **159**, 1237 (1968).
6. V. V. Reshetnyak, *Tr. Zool. Inst. Akad. Nauk SSSR* **53**, 785 (1974).
7. S. Honjo, *J. Mar. Res.* **36**, 469 (1978); *ibid.* **38**, 53 (1980).
8. K. Takahashi and S. Honjo, *Micropaleontology* **27**, 140 (1981); K. Takahashi, thesis, Massachusetts Institute of Technology–Woods Hole Oceanographic Institute (1981); *Woods Hole Oceanogr. Inst. Tech. Rep. 81–103* (1981); in *Ocean Biocoenosis*, S. Honjo, Ed. (Micropaleontology Press, New York, in press).
9. A. P. Lisitzin, *Sedimentation in the World Ocean* (Special Publication 17, Society of Economic Paleontologists and Mineralogists, Tulsa, Okla., 1972).
10. We used a 100-μm-mesh plankton net (0- to 100-m night vertical tow); specimens were immediately rinsed and dried on board.
11. K. Takahashi and S. Honjo, *Deep-Sea Res.* **30**, 543 (1983).
12. D. S. Lowson, D. C. Hurd, H. S. Pankratz, *Am. J. Sci.* **278**, 1373 (1978); D. C. Hurd and S. Birdwhistell, *ibid.* **283**, (1983); D. C. Hurd *et al.*, *ibid.* **281**, 833 (1981).
13. Diameter, 407 ± 59 μm (N = 32); weight, 9.7 ± 3.6 μg (N = 125).
14. T. C. Moore, Jr., *Geol. Soc. Am. Bull.* **80**, 2103 (1969).
15. F. R. Kunze and R. E. Casey, *Geol. Soc. Am. Abstr. Programs* **12** (No. 7), 467 (1980).
16. We thank V. Asper and S. Houghton for transmission electron microscopy. The Deep Sea Drilling Project, supported by the National Science Foundation, provided the core samples. We thank W. R. Riedel, B. Corliss, and G. P. Lohman for critical reviews of the manuscript. This study was supported by NSF grants OCE 80-19386 and OCE 82-08638. This is Woods Hole Oceanographic Institution Contribution Number 5280.

3 December 1982; accepted 6 July 1983